HEAT TRANSFER AND CROSS-DIFFUSION DUE TO A SPHERE OF CONSTANT THERMAL ENERGY EMBEDDED IN A POROUS MEDIUM

by

Appavuraj MOHAN[a]* and Renganathan GANAPATHY[b]

[a] Department of Mathematics, Urumu Dhanalakshmi College, Trichirappalli, India
[b] Faculty of Sciences, MAM College of Engineering, Trichy, India

Original scientific paper
https://doi.org/10.2298/TSCI17S2503M

Heat transfer and cross-diffusion due to a sphere of constant thermal energy and concentration embedded in unbounded homogeneous porous medium in a regime where the temperature gradient produces mass flux is analytically studied using Darcy flow model. Analytical solution is obtained with regular perturbation analysis in the limit of small Rayleigh number. Due to cross-diffusion, solute front initially shows stronger convection than thermal front, but ultimately reaches steady-state at approximately the same time as that of thermal front. Quantity of heat necessary to maintain the steady-state is found to be least near the rear stagnation point and the mean Nusselt number is found to be unaffected by cross-diffusion. Nusselt number variation for different cone angles and Soret number is studied and it is found that higher improvement is achieved when cone angle is changed from 80 to 100°.

Key words: *thermal energy, thermo-diffusion, Darcy flow, porous medium, sphere*

Introduction

Heat transfer due to the presence of heat sources in saturated porous media has been the subject of study in recent years in view of its wide ranging applications to a variety of fields such as in the storage of thermal energy, and in the management of nuclear waste to mention but a few. However, in most practical situations, species concentration gradients greatly affect the flow and as a result, they play a decisive role in the development of thermal fields, such as migration of moisture in fibrous insulations, spreading of pollutants in water saturated soil and in underground disposal of nuclear waste. When the temperature gradient is steep, cross-coupling between thermal and solutal diffusions are no longer negligible and presumably for this reason, Soret effect is being widely considered for isotope separation and in mixture of gases of light and medium molecular weights [1]. In fact, the importance of thermo-diffusion, though considered as a second-order phenomenon, is becoming more widely accepted in a variety of fields that includes mineral enrichment of geothermal sources, hydrocarbon separation in petrology and magma differentiation in geosciences, besides others [2].

Analytical studies on double-diffusive convection in a horizontal fluid-saturated porous layer, heated and salted from below in the presence of Soret and Dufour effects, using linear and non-linear stability analyses is done by Malashetty and Biradar [3]. In natural con-

* Corresponding author, e-mail: appavumohan@gmail.com

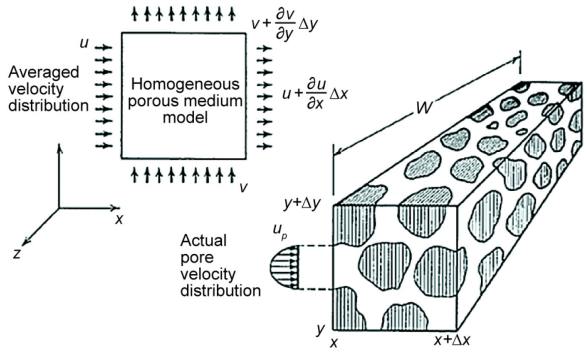

Figure 1. Model of porous medium

vection heat and mass transfer of non-Darcy porous medium, presence of Soret effect reduces the dependence of volume flow rate and heat rate on the modified Darcy number [4]. Soret effect is very much important with the presence of gravity vector drives a strong connection with inclusion of thermal diffusion in porous cavity [5]. Motivated by the significance of understanding thermo-diffusion in energy storage and nuclear waste management, Ganapathy and Mohan [6] investigated the phenomenon around a concentrated source embedded in an unbounded porous medium, assuming the validity of the Darcy flow model. The problem discussed by them models the situation wherein a small but a finite volume inside a much larger porous medium is suddenly heated. The research gap identified from the literature survey is, that the heat source is finite it would be more appropriate to model the situation with a sphere of constant thermal energy and concentration. Further, we assume that the validity of the Darcy flow model and obtain an analytical solution of the problem using a regular perturbation analysis in the limit of small Rayleigh numbers in a regime where the temperature gradient produces mass flux as well. The relationship between the Soret number and cone angle is also investigated and the influence of Nusselt number is studied. Figure 1 shows the model of pore velocity distribution on homogenous porous medium.

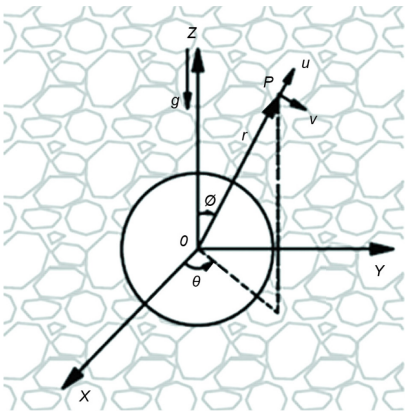

Figure 2. Physical set-up of the problem. Configuration of interest: spherical-polar co-ordinate system (r, φ, θ) with the origin at the center of the sphere

Mathematical formulation

Free convective heat and mass transfer Darcy flow with thermal diffusion around a sphere of radius a of constant thermal energy Q [W] and species generation rate m [kgs^{-1}] embedded instantaneously in an unbounded porous medium of low permeability is considered in this work. The medium is assumed to be rigid, homogeneous and isotropic and the fluid saturating the medium Boussinesq incompressible with the density-temperature-concentration relation:

$$\rho = \rho_\infty[1-\beta(T-T_\infty)-\beta_C(C-C_\infty)] \qquad (1)$$

where the symbols have their usual meanings (see nomenclature). We use a spherical-polar co-ordinate system (r, φ, θ) with the origin at the center of the sphere and the axis $\varphi = 0$ vertically upwards and parallel but opposite to the gravity vector (fig. 2). The assumptions made are as follows.

– The fluid and the porous structure are assumed to be in local thermal equilibrium.
– The medium is homogeneous.

– The medium is isotropic, meaning that transport properties do not depend on the direction of the experiment.
– At any point in the porous medium, the solid matrix is in thermal equilibrium with the fluid filling the pores.
– The local Reynolds number based on averaged velocity and $K^{1/2}$ does not exceed the range 1-10, meaning that the Darcy law applies in its original form.

Thus, with the Darcy flow model, we have for the conservation of mass, momentum, energy, and species concentration with thermo-diffusion and in the absence of dispersion.

$$\nabla\vec{\mathrm{q}} = 0 \tag{2}$$

$$\vec{\mathrm{q}} = -\left(\frac{K}{\mu}\right)(\nabla P + \rho g\vec{\mathrm{n}}) \tag{3}$$

$$\sigma\frac{\partial T}{\partial t} + (\vec{\mathrm{q}}\nabla)T = \alpha\Delta T \tag{4}$$

$$\varepsilon\frac{\partial C}{\partial t} + (\vec{\mathrm{q}}\nabla)C = \Delta(D_m C + D_{CT}T) \tag{5}$$

In writing the above equations we have assumed that the medium and the saturating fluid are in thermal equilibrium, the thermo-diffusion coefficient is not excessive and that all physical quantities are constant except in the buoyancy term [7]. Taking note of spherical symmetry in the angular direction θ and making use of eq. (2), we define a stream function ψ such that:

$$\vec{\mathrm{q}} = \left(\frac{1}{r^2\sin\varphi}\frac{\partial\psi}{\partial\varphi},\quad -\frac{1}{r\sin\varphi}\frac{\partial\psi}{\partial r},\quad 0\right) \tag{6}$$

and introduce the non-dimensional quantities:

$$R = \frac{r}{L},\quad \tau = \frac{\alpha t}{\sigma L^2},\quad \Psi = \frac{\psi}{\alpha L},\quad \Theta = \left(\frac{k}{L}\right)\frac{(T-T_\infty)}{Q},\quad C^* = \left(\frac{D_m}{L}\right)\frac{(C-C_\infty)}{m} \tag{7}$$

to obtain for the conservation of momentum, energy and species concentration:

$$\frac{1}{R^2}\left(\frac{\partial}{\partial\varphi}\right)\left(\frac{1}{\sin\varphi}\frac{\partial\Psi}{\partial\varphi}\right) + \frac{1}{\sin\varphi}\left(\frac{\partial^2\Psi}{\partial R^2}\right) =$$
$$= \mathrm{Ra}\left[\left(\cos\varphi\frac{\partial\Theta}{\partial\varphi} + R\sin\varphi\frac{\partial\Theta}{\partial R}\right) + N\left(\cos\varphi\frac{\partial C}{\partial\varphi} + R\sin\varphi\frac{\partial C}{\partial R}\right)\right] \tag{8}$$

$$\frac{\partial\Theta}{\partial\tau} + \left(\frac{1}{R^2\sin\varphi}\right)\frac{\partial(\Psi,\Theta)}{\partial(\varphi,R)} = \frac{1}{R^2}\left[\frac{\partial}{\partial R}\left(R^2\frac{\partial\Theta}{\partial R}\right) + \frac{1}{\sin\varphi}\frac{\partial}{\partial\varphi}\left(\sin\varphi\frac{\partial\Theta}{\partial\varphi}\right)\right] \tag{9}$$

$$A^2\frac{\partial C}{\partial\tau} + \mathrm{Le}\left(\frac{1}{R^2\sin\varphi}\right)\frac{\partial(\Psi,C)}{\partial(\varphi,R)} = \frac{1}{R^2}\left[\frac{\partial}{\partial R}\left(R^2\frac{\partial C}{\partial R}\right) + \frac{1}{\sin\varphi}\frac{\partial}{\partial\varphi}\left(\sin\varphi\frac{\partial C}{\partial\varphi}\right)\right] +$$
$$+\frac{\lambda}{R^2}\left[\frac{\partial}{\partial R}\left(R^2\frac{\partial\Theta}{\partial R}\right) + \frac{1}{\sin\varphi}\frac{\partial}{\partial\varphi}\left(\sin\varphi\frac{\partial\Theta}{\partial\varphi}\right)\right] \tag{10}$$

where, $A^2 = [(\varepsilon/\sigma)\mathrm{Le}]$ and the Soret number, λ, is related to the Soret coefficient by:

$$\lambda = D_{CT}\left(\frac{Q}{km}\right) \tag{11a}$$

and

$$\frac{\partial(p,q)}{\partial(x,y)} = \frac{\partial p}{\partial x}\frac{\partial q}{\partial y} - \frac{\partial p}{\partial y}\frac{\partial q}{\partial x} \tag{11b}$$

is the Jacobian. The asterisk in C is dropped for convenience. Though it is customary to use the radius of the sphere as the characteristic length scale, we have so chosen L that the solution for the analogous problem that treats a concentrated point source could be deduced algebraically from the results of the present study using an appropriate analytical technique [8]. The initial and boundary conditions in non-dimensional formulation are:

$$U, V, \Theta, C = 0 \quad \text{when} \quad \tau = 0 \tag{12a}$$

$$U, V, \Theta, C \to 0 \quad \text{as} \quad R \to \infty \tag{12b}$$

$$\frac{\partial U}{\partial \varphi} = V = \frac{\partial \Theta}{\partial \varphi} = \frac{\partial C}{\partial \varphi} = 0 \quad \text{at} \quad \varphi = 0, \pi \quad \text{when } R = R_0 \tag{12c}$$

where, $R_0 = a/L$ and $(U, V) = (L/\alpha)(u, v)$. For the heat and concentration balance we have:

$$\lim_{R\to R_0}\left(\frac{\partial \Theta}{\partial R}\right) = -1, \quad \lim_{R\to R_0}\left(\frac{\partial C}{\partial R}\right) = -1 \tag{13}$$

Method of solution

We seek a perturbation solution by assuming power series expansions of the form:

$$(\Psi, \Theta, C)(R, \varphi, \tau; R_0) = \sum_{n=0}^{\infty} \mathrm{Ra}^n (\Psi_n, \Theta_n, C_n)(R, \varphi, \tau; R_0) \tag{14}$$

and substitute eq. (14) into eqs. (8)-(10) to collect terms of equal powers in Ra for the determination of the various order solutions. As the zero-order solution corresponds to a state of thermal conduction, there is no fluid motion and hence without any loss one may take $\Psi_0 = 0$. The functions Θ_0 and C_0 are then found from the solutions of the equations:

$$\frac{\partial \Theta_0}{\partial \tau} = \frac{1}{R^2}\left[\frac{\partial}{\partial R}\left(R^2 \frac{\partial \Theta_0}{\partial R}\right)\right] \tag{15a}$$

$$A^2 \frac{\partial C_0}{\partial \tau} = \frac{1}{R^2}\left[\frac{\partial}{\partial R}\left(R^2 \frac{\partial C_0}{\partial R}\right)\right] + \frac{\lambda}{R^2}\left[\frac{\partial}{\partial R}\left(R^2 \frac{\partial \Theta_0}{\partial R}\right)\right] \tag{15b}$$

in which by setting

$$\Theta_0 = R^{-1}G(R,\tau), \quad C_0 = R^{-1}H(R,\tau) \tag{16}$$

one obtains after taking the Laplace transform:

$$\ell[G(R,\tau)] = R_0^2 \left\{ \frac{1}{s(1+R_0\sqrt{s})} \exp[-(R-R_0)\sqrt{s}] \right\} \tag{16a}$$

$$\ell[H(R,\tau)] = R_0^2 \left\{ \frac{(1+\omega)}{s(1+AR_0\sqrt{s})} \exp[-A(R-R_0)\sqrt{s}] - \frac{\omega}{s(1+R_0\sqrt{s})} \exp[-(R-R_0)\sqrt{s}] \right\} \tag{16b}$$

where $\omega = \lambda/(1-A^2)$.

Using the table of Laplace transforms by Campbell and Foster [9], we have after inversion:

$$\Theta_0 = F(\eta,\eta_0) \tag{17a}$$

$$C_0 = [(1+\omega)F(A\eta, A\eta_0) - \omega F(\eta,\eta_0)], \quad (A \neq 1) \tag{17b}$$

$= F(\eta, \eta_0)$

$$+\frac{\lambda R_0}{4\eta_0^2}\left(\frac{\eta_0}{\eta}\right)\left[\frac{2}{\sqrt{\pi}}\eta_0 \exp[-(\eta-\eta_0)^2] + \exp\left(\frac{\eta}{\eta_0}-1+\frac{1}{4\eta_0^2}\right)\operatorname{erfc}\left(\eta-\eta_0+\frac{1}{2\eta_0}\right)\right], \quad (A=1) \tag{17c}$$

and

$$F(\eta,\eta_0) = R_0\left(\frac{\eta_0}{\eta}\right)\left[\operatorname{erfc}(\eta-\eta_0) - \exp\left(\frac{\eta}{\eta_0}-1+\frac{1}{4\eta_0^2}\right)\operatorname{erfc}\left(\eta-\eta_0+\frac{1}{2\eta_0}\right)\right] \tag{18}$$

erfc(·) being the complementary error function.

The first convective correction to the flow field is now found from the solution of the equation:

$$\frac{1}{R^2}\frac{\partial}{\partial\varphi}\left(\frac{1}{\sin\varphi}\frac{\partial\Psi_1}{\partial\varphi}\right) + \frac{1}{\sin\varphi}\left(\frac{\partial^2\Psi_1}{\partial R^2}\right) = R\sin\varphi\left[\left(\frac{\partial\Theta_0}{\partial R}\right) + N\left(\frac{\partial C_0}{\partial R}\right)\right] \tag{19}$$

in which the separation of the variables is achieved by setting:

$$\Psi_1 = 2\sqrt{\tau}R_0^2\sin^2\varphi f(\eta,\eta_0) \tag{20}$$

This then yields for the determination of $f(\eta, \eta_0)$:

$$\eta^2\frac{\mathrm{d}^2 f}{\mathrm{d}\eta^2} - 2f = (1-N\omega)\chi(\eta,\eta_0) + \left(\frac{N}{A^2}\right)(1+\omega)\chi(A\eta, A\eta_0) \tag{21}$$

where

$$\chi(\eta,\eta_0) = -\eta^2\left[\left(\frac{\eta_0}{\eta}\right)\operatorname{erfc}(\eta-\eta_0) + \left(1-\frac{\eta_0}{\eta}\right)\exp\left(\frac{\eta}{\eta_0}-1+\frac{1}{4\eta^2}\right)\operatorname{erfc}\left(\eta-\eta_0+\frac{1}{2\eta_0}\right)\right] \tag{22}$$

Solution of eq. (21) is found to be:

$$f(\eta,\eta_0) = (1-N\omega)\xi(\eta,\eta_0) + \left(\frac{N}{A}\right)(1+\omega)\xi(A\eta, A\eta_0), \quad (A \neq 1) \tag{23a}$$

$$= (1+N)\xi(\eta,\eta_0) + \tfrac{1}{2}N\lambda\Omega(\eta,\eta_0), \quad (A=1) \tag{23b}$$

where

$$\xi(\eta,\eta_0) = -\eta_0\left(1-\frac{\eta_0}{\eta}\right)\exp\left(\frac{\eta}{\eta_0}-1+\frac{1}{4\eta_0^2}\right)\operatorname{erfc}\left(\eta-\eta_0+\frac{1}{2\eta_0}\right)+\left(\frac{1}{2}\right)\eta_0\left(\frac{\eta}{\eta_0}-\frac{\eta_0}{\eta}\right)\operatorname{erfc}(\eta-\eta_0)+$$
$$+\left(\frac{1}{4\eta}\right)\operatorname{erf}(\eta-\eta_0)-\left(\frac{1}{2\sqrt{\pi}}\right)\left(1-\frac{\eta_0}{\eta}\right)\exp[-(\eta-\eta_0)^2] \tag{23c}$$

and

$$\Omega(\eta,\eta_0) = -\eta_0\left[2\left(1-\frac{\eta_0}{\eta}\right)-\frac{\eta}{\eta_0}\right]\exp\left(\frac{\eta}{\eta_0}-1+\frac{1}{4\eta_0^2}\right)\operatorname{erfc}\left(\eta-\eta_0+\frac{1}{2\eta_0}\right)-$$
$$-\eta_0\left(\frac{\eta_0}{\eta}\right)\operatorname{erfc}(\eta-\eta_0)+\left(\frac{1}{2\eta}\right)\operatorname{erf}(\eta-\eta_0)-\frac{1}{\sqrt{\pi}}\left(1-\frac{\eta_0}{\eta}\right)\exp[-(\eta-\eta_0)^2] \tag{23d}$$

Discussion

While ω determines the Soret effect, the parameter A, being the ratio of thermal penetration length $O[(\alpha\tau/\sigma)^{1/2}]$ to that of species penetration $O[(D_m\tau/\varepsilon)^{1/2}]$, determines the impact of the species concentration gradients upon the thermally driven flow. In order to demonstrate the effect of cross-diffusion on heat transfer, contours of the transient streamlines Ψ_1/Ra= constant are drawn at a common time τ = 0.5 (fig. 3) for two different values of ω choosing in illustration R_0 = 1, A = 0.4, N = –0.4.The choice of A is justified, since in the case of diffusion of methanol and hydrogen in water saturated glass beads, $A \approx 0.36$. Likewise when the two buoyancy mechanisms are opposed, N is negative and for simplicity we have so chosen N that N/A = –1. Obviously, in the early stages of flow development, counter rotating cells are formed with those in the colder front rotating anti-clockwise giving rise to a downward flow and that the colder front showing stronger convection than the thermal front. Consequently, the volume of the region, in which the thermal effect of the sphere is felt, is significantly reduced, the reduction in volume being about 13.9% when λ = 0.252, that is, when ω = 0.3 and the stagnation points of

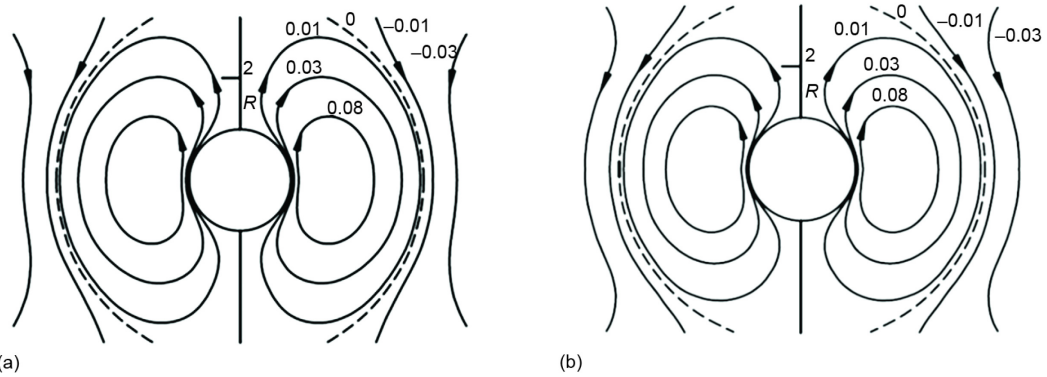

Figure 3. Transient streamlines Ψ_1/Ra = constant for various values of ω (R_0 = 1, A = 0.4, N = –0.4, τ = 0.5); (a) ω = 0, (b) ω = 0.3

the flow field are found to be at $R = 1.96, 1.89$ when $\omega = 0, 0.3$, respectively. From the maps of streamlines drawn in fig. 4 one may observe that as time increases the geometry of the flow pattern changes. Initially the thermal front moves faster than the solute front but ultimately they both reach the steady-state at approximately the same time. Consequently, for very large times, the dual counter rotating cells break down into a single cell. The temperature and species concentration decrease outward from the sphere in all directions with symmetry about the horizontal plane through the origin. Most of these results are in conformity with the observations put forth by Nejad *et al.* [5]. As our study is primarily concerned with a single component chemical species in a single phase fluid and as migration of fluid particles is from the hotter region to the colder one, the Soret parameter assumes only positive values.

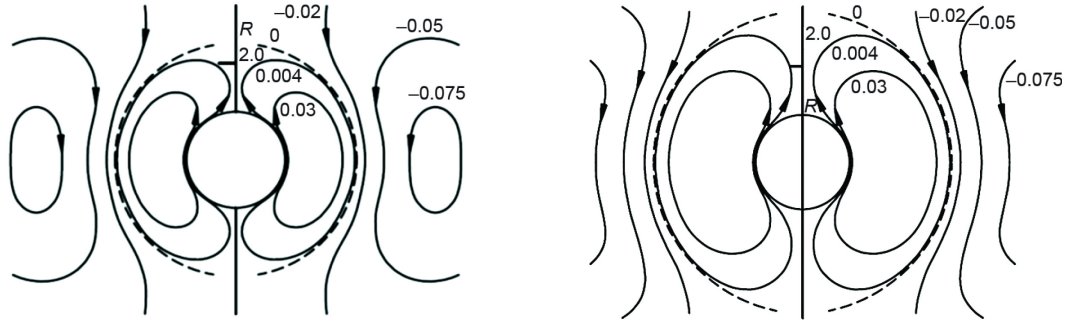

Figure 4. Transient streamlines Ψ_1/Ra = const. for various values of τ($R_0 = 1$, $A = 0.4$, $N = -0.4$, $\omega = 0.5$); (a) $\tau = 0.2$, (b) $\tau = 0.4$

As the algebra is overwhelming, the higher-order convective corrections thermal and concentration fields could not be determined. However, the error due to the non-inclusion of these terms is not of great physical significance [10]. One may observe that in the limit $N \to 0$, we recover the results of Sano and Okihara [11], of course, with a different non-dimensionalization scheme.

Steady-state

Since the method of solution is straight forward, we present only the final results. In what follows, ζ represents R/R_0. Thus, with the same notations as before we have:

$$\Psi = \mathrm{Ra}\left(\frac{R_0^{\,3}}{2}\right)(1+N)(\zeta-\zeta^{-1})\sin^2\varphi$$

$$+\mathrm{Ra}\left(\frac{R_0^{\,5}}{2}\right)(1+N)[1+N(\mathrm{Le}-\lambda)]\left(\frac{1}{3}\zeta-\frac{5}{8}+\frac{1}{2}\zeta^{-1}-\frac{5}{24}\zeta^{-2}\right)\sin^2\varphi\cos\varphi+O(\mathrm{Ra}^3) \quad (24)$$

$$\Theta = R_0\zeta^{-1}+\mathrm{Ra}\left(\frac{R_0^3}{2}\right)(1+N)\left(\zeta^{-1}-\frac{5}{4}\zeta^{-2}+\frac{1}{2}\zeta^{-3}\right)\cos\varphi+$$

$$+\mathrm{Ra}^2\left(\frac{R_0^{\,5}}{4}\right)(1+N)\{(1+N)(Y_1+Y_2\cos 2\varphi)+[1+N(\mathrm{Le}-\lambda)](Z_1+Z_2\cos 2\varphi)\}+O(\mathrm{Ra}^3) \quad (25)$$

$$C = R_0\zeta^{-1} + \mathrm{Ra}\left(\frac{R_0^{\,3}}{2}\right)(1+N)(\mathrm{Le}-\lambda)\left(\zeta^{-1} - \frac{5}{4}\zeta^{-2} + \frac{1}{2}\zeta^{-3}\right)\cos\varphi +$$
$$+\mathrm{Ra}^2\left(\frac{R_0^{\,5}}{4}\right)(1+N)\{(1+N)[\mathrm{Le}(\mathrm{Le}-\lambda)-\lambda](Y_1 + Y_2\cos 2\varphi) +$$
$$+(1+N)[\mathrm{Le}(\mathrm{Le}-\lambda)-\lambda](Y_1 + Y_2\cos 2\varphi) +$$
$$+(\mathrm{Le}-\lambda)[1+N(\mathrm{Le}-\lambda)](Z_1 + Z_2\cos 2\varphi) + O(\mathrm{Ra}^3) \tag{26}$$

where

$$Y_1 = -\frac{7}{12}\zeta^{-1} + \frac{5}{32}\zeta^{-2} + \frac{377}{1008}\zeta^{-3} + \frac{1}{12}\zeta^{-3}\ln R - \frac{5}{16}\zeta^{-4} + \frac{27}{280}\zeta^{-5}$$
$$Y_2 = \frac{1}{4}\zeta^{-1} - \frac{25}{32}\zeta^{-2} + \frac{265}{336}\zeta^{-3} + \frac{1}{4}\zeta^{-3}\ln R - \frac{5}{16}\zeta^{-4} + \frac{5}{56}\zeta^{-5}$$
$$Z_1 = \frac{1}{18}\zeta^{-1} - \frac{5}{32}\zeta^{-2} + \frac{157}{2160}\zeta^{-3} + \frac{1}{10}\zeta^{-3}\ln R + \frac{5}{144}\zeta^{-4}$$
$$Z_2 = \frac{1}{6}\zeta^{-1} - \frac{15}{32}\zeta^{-2} + \frac{157}{720}\zeta^{-3} + \frac{3}{10}\zeta^{-3}\ln R + \frac{5}{48}\zeta^{-4} \tag{27a-d}$$

In the absence of cross-diffusion, one may recover the results of Lai and Kulacki [12] with $R_0 = 1$. It is observable from fig. 5, that more closer the streamline to the vertical is, the more wid apart it is from the vertical in the lower half space with the phenomenon getting more pronounced with increasing λ. This then implies that the momentum transfer is retarded in the colder front than on the thermal front. Likewise, profiles of the steady-state isotherms and lines of constant concentration (fig. 6) show that larger the value of λ is, greater is the shift of the warm and high concentration region below the sphere. Asan essential characteristic of heat transfer, we evaluate the Nusselt number given by:

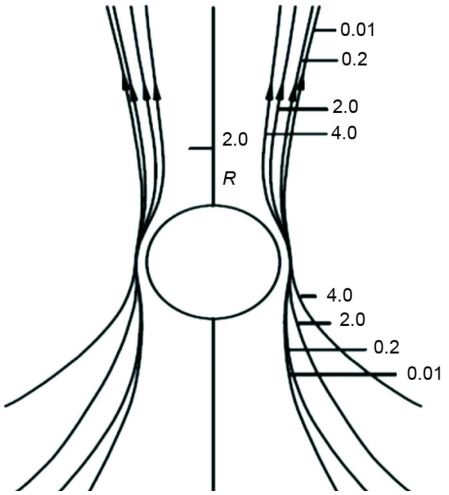

Figure 5. The effect of the Soret parameter on the steady-state streamlines Ψ/Ra = 0.4 (R_0 = 1, Le = 2.0, N = -0.4, Ra = 3); numbers on the graph represent values of λ

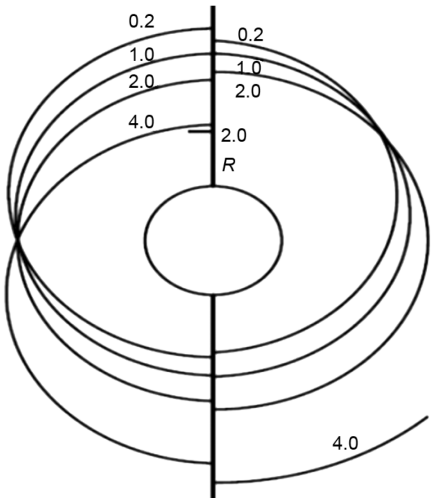

Figure 6. Profiles of isotherms Θ = 0.3 (left side) and lines of constant concentration C = 0.3 (right side) (R_0 = 1, Le = 2.0, N = -0.4, Ra = 3); NUMBERS on the graphs represent values of λ

$$\mathrm{Nu} = \lim_{r \to a}\left[\frac{a}{k}\frac{Q}{(T - T_\infty)}\right] \tag{28}$$

which in non-dimensional form reduces to:

$$\mathrm{Nu} = \lim_{R \to R_0}\left(\frac{R_0}{\Theta}\right) \tag{28a}$$

With a three-term approximation of Θ, we have:

$$\mathrm{Nu} = 1 - \frac{R_0^2}{8}(1+N)\cos\varphi\,\mathrm{Ra} + \frac{R_0^4}{40320}(1+N)^2\left[(3028 - 30\cos 2\varphi) - \right.$$
$$\left. -203\frac{1+N(\mathrm{Le}-\lambda)}{1+N}\left(\frac{1}{3} + \cos 2\varphi\right)\right]\mathrm{Ra}^2 \tag{29}$$

and the mean Nusselt number averaged over the surface of the sphere is found to be:

$$\mathrm{Nu}_{\mathrm{ave}} = \frac{1}{2}\int_0^\pi \mathrm{Nu}\sin\varphi\,\mathrm{d}\varphi = 1 + \frac{217}{2880}R_0^4(1+N)^2\,\mathrm{Ra}^2 \tag{30}$$

It is observable from tab. 1 that Nu is a minimum when $\varphi = 0$ and as φ increases, Nu increases monotonically so that the quantity of heat necessary for the maintenance of the steady-state is least near the rear stagnation point than elsewhere, and the phenomenon is more pronounced with increasing values of λ. However, one may observe from the same table that there is a dip in the value of Nu as λ assumes values greater than one. We find that the mean Nusselt number is independent of the Soret effect. Figure 7 shows the variation of Nusselt number for different cone angles and for different soret number. It is observed that, from 0 to 40° and from 140 to 180° cone angle, for different Soret number, a significant variation in Nusselt number is seen. But in between 40 to 140° cone angle, for all Soret numbers, there is no much different in Nusselt number. A sharp increase in Nusselt number is experienced between 40 to 140° cone angles. Higher Nusselt number is observed with 0.1 soret number.

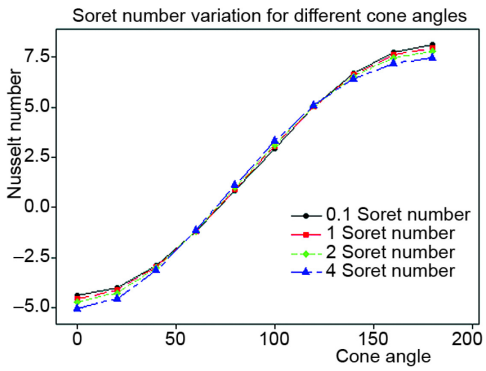

Figure 7. Variation of Nusselt number for different Soret number

Table 1. Values of 100 (Nu – 1) for increasing values of λ (N = –0.05, Ra = 1, Le = 2.0)

φ / λ	0	$\frac{\pi}{9}$	$2\frac{\pi}{9}$	$3\frac{\pi}{9}$	$4\frac{\pi}{9}$	$5\frac{\pi}{9}$	$6\frac{\pi}{9}$	$7\frac{\pi}{9}$	$8\frac{\pi}{9}$	π
0.1	–4.408	–4.024	–2.920	–1.236	0.817	2.908	5.014	6.656	7.722	8.097
1.0	–4.599	–4.148	–2.977	–1.217	0.886	3.057	5.033	6.598	7.598	7.941
2.0	–4.727	–4.287	–3.047	–1.196	0.967	3.113	5.054	6.534	7.460	7.773
4.0	–5.062	–4.563	–3.169	–1.154	1.115	3.286	5.096	6.407	7.183	7.438

Conclusion

Assuming the Darcy flow model, phenomenon of thermal convection and the effect of cross-diffusion due to a heated sphere embedded instantaneously in a porous medium is investigated analytically. From the analysis we deduce that cross-diffusion is found to inhibit heat transfer. Further, due to cross-diffusion, there is a reduction in the volume of the region in which the thermal effect is felt and that there is retardation in the rate of momentum transfer in the colder front than on the thermal front. There is a monotonic decrease in the heat transfer rate as Soret number increases and the quantity of heat necessary to maintain the steady-state is found to be least near the rear stagnation point than elsewhere. The mean Nusselt number remains unaffected by cross-diffusion.

Nomenclature

A – non-dimensional parameter, $\{= [(\varepsilon/\sigma)\mathrm{Le}]^{1/2}\}$
a – radius of the sphere, [m]
C – the species concentration
C^* – species concentration, [–]
D_{CT} – Soret coefficient
D_m – solutal diffusivity
K – porous medium permeability, [m^2]
k – thermal conductivity of the fluid-porous matrix, [$kgms^{-3}K^{-1}$]
ℓ – Laplace transform
L – characteristic length scale
Le – Lewis number, $(= \alpha/D_m)$
m – species generation rate, [kgs^{-1}]
N – buoyancy ratio $\{= [\beta_c mk/(\beta Q D_m)]\}$
Nu – Nusselt number
Nu_{ave} – mean Nusselt number
$\vec{n}$ – unit vector in the vertical direction
Q – thermal energy of the sphere, [W]
R – non-dimensional radial co-ordinate
Ra – thermal Rayleigh number, $[= (\beta gK)/(\alpha \nu k)]QL$
R_0 – non-dimensional radius of the sphere $(= a/L)$
r – radial co-ordinate, [m]
T – temperature, [K]
t – time, [s]
u – radial velocity
V – non-dimensional form of the transverse velocity
v – transverse velocity, [ms^{-1}]
$Y_{1,2}$ – functions of ζ (eq. 27a-b)
$Z_{1,2}$ – functions of ζ (eq. 27c-d)

Greek symbols

α – effective thermal diffusivity of the fluid-porous matrix
β – thermal expansion coefficient
β_C – solutal expansion coefficient
ε – porosity of the porous matrix
ζ – non-dimensional variable, R/R_0
η – similarity variable, $R/2\sqrt{\tau}$
η_0 – similarity variable, $R_0/2\sqrt{\tau}$
Θ – non-dimensional temperature
θ – polar angle
λ – Soret number, $D_{CT}(Q/km)$
μ – coefficient of viscosity of the fluid
ν – kinematic viscosity of the fluid
ξ – function of (η, η_0), eqn.(23c)
ρ – fluid density
σ – heat capacity ratio, $\varepsilon + (1 - \varepsilon)(\rho c_p)_s/(\rho c_p)_f$
τ – non-dimensional time
φ – cone angle
χ – function of (η, η_0), eq. (22)
Ψ – non-dimensional stream function
Ω – function of (η, η_0), eq. (23d)
ω – non-dimensional parameter, $\lambda/(1 - A^2)$

Subscripts

f – fluid phase
s – solid phase
∞ – reference state
n – n^{th} term (n = 0, 1, 2,..)

References

[1] Melly, L. B. B., *et al.,* Modeling Soret Coefficient Measurement Experiments in Porous Media Considering Thermal and Solutal Convection, *International Journal of Heat & Mass Transfer*, *44* (2001), 7, pp. 1285-1297

[2] Bahloul, A., *et al.,* Double Diffusive and Soret Induced Convection in a Shallow Horizontal Porous Layer, *Journal of Fluid Mechanics, 491* (2003), Aug., pp. 325-352
[3] Malashetty, M. S., Biradar, B. S., Linear and Nonlinear Double-Diffusive Convection in a Fluid-Saturated Porous Layer with Cross-Diffusion Effects, *Transport in Porous Media*, *91* (2012), 2, pp. 649-675
[4] Jha, B. K., *et al.,* Diffusion-Thermo Effects on Free Convective Heat and Mass Transfer Flow in a Vertical Channel with Symmetric Boundary Conditions, *Journal of Heat Transfer, 133* (2011), 5, pp. 1-8
[5] Nejad, M., *et al.,* Role of Thermal Diffusion on Heat and Mass Transfer in Porous Media, *International Journal of Computational Fluid Dynamics, 15* (2001), 2, pp. 157-168
[6] Ganaparthy, R., Mohan, A., Thermo-Diffusive Darcy Flow Induced by a Concentrated Source, *Ain Shams Engineering Journal*, *7* (2016), 4, pp. 1069-1078
[7] Nield, D. A., Bejan, A. *Convection in Porous Media*, Springer-Verlag, New York, 2013
[8] Hickox, C. E. Thermal Convection at Low Rayleigh Number from Concentrated Sources in Porous Media, *ASME Journal of Heat Transfer, 103* (1981), 2, pp. 232-236
[9] Campbell, G. A., Foster, R. M., *Fourier Integrals for Practical Applications*, Van Nostrand, New York, USA, 1961
[10] Ganapathy, R., Purushothaman, R., Free Convection in an Infinite Porous Medium Induced by a Heated Sphere, *International Journal of Engineering Science, 28* (1990), 8, pp. 751-759
[11] Sano, T., Okihara, T. R., Natural Convection around a Sphere Immersed in a Porous Medium at Small Rayleigh Numbers, *Fluid Dyn. Res*., *13* (1994), 1, pp. 39-44
[12] Lai, P. C., Kulacki, F. A., Coupled Heat and Mass Transfer from a Sphere Buried in an Infinite Porous Medium, *International Journal of Heat & Mass Transfer, 33* (1990), 1, pp. 209-215

Paper submitted: May 15, 2017
Paper revised: August 8, 2017
Paper accepted: August 22, 2017